ISSN 0021-8944, Journal of Applied Mechanics and Technical Physics, 2020, Vol. 61, No. 1, pp. 87–100. © Pleiades Publishing, Ltd., 2020.
Original Russian Text © I.A. Banshchikova.

CONSTRUCTION OF CONSTITUTIVE EQUATIONS FOR ORTHOTROPIC MATERIALS WITH DIFFERENT PROPERTIES IN TENSION AND COMPRESSION UNDER CREEP CONDITIONS

I. A. Banshchikova*

UDC 539.376

Abstract: Constitutive steady-state creep equations are proposed for orthotropic materials with different tensile and compressive resistances. The resistances are described using lower functions with different exponents for tension and compression. Equations are written for tension, shear, and plane stress problems. The model is used to solve the problem of torsion by a constant moment at a temperature $T = 200°C$ for annular cross-section rods cut from a plate of AK4-1 transversely isotropic alloy in the normal direction to the plate and in the longitudinal direction. Constitutive equations for torsion are derived. Values of model parameters were obtained in experiments on uniaxial tension and compression of solid circular specimens cut in various directions. An analytical solution for the rate of torsion angle of a circular cross-section rod cut normal to the plate was obtained for the same exponent in tension and compression. For a rod cut in the longitudinal direction, an upper estimate of the torsion angle rate was obtained. The calculated results are in satisfactory agreement with experimental data.

Keywords: structural alloys, orthotropy, different resistance in tensile and compression, creep, plane stress state, shear, torsion of circular cross-section rods, additional dissipation power.

DOI: 10.1134/S0021894420010101

INTRODUCTION

Generally, modern structural alloys have anisotropy properties at high temperatures. The properties of blank sheet materials may vary in the plane of the sheet, normal to it, and in a direction at an angle of 45° to the sheet normal. Anisotropy of this type may be due to blank rolling. In addition to anisotropy, materials can have different properties in tension and compression. There are a number of models that describe the deformation of such materials under creep conditions.

Models describing isotropic materials with different properties in tension and compression under creep conditions use, as a rule, power functions with the same [1–4] or different [5–7] exponents in tension and compression. The torsion of solid circular specimens using two such models [1, 5] based on the concept of transformed stress space is analyzed in [8].

Models of anisotropic materials whose tensile and compressive properties are assumed to be the same were proposed in [9, 10]. Sosnin [9], using a model similar to the Hill anisotropic plasticity model, developed an orthotropic model that uses a function with the same exponent to describe material properties in different directions. Betten [10]

Lavrent'ev Institute of Hydrodynamics, Siberian Branch, Russian Academy of Sciences, Novosibirsk, 630090 Russia; *binna@ngs.ru. Translated from Prikladnaya Mekhanika i Tekhnicheskaya Fizika, Vol. 61, No. 1, pp. 102–117, January–February, 2020. Original article submitted March 6, 2019; revision submitted April 29, 2019; accepted for publication July 29, 2019.

*Corresponding author.

considered a model in which the properties of an orthotropic material are described using a function with different exponents in the three principal directions of orthotropy.

Anisotropic material models that take into account the difference in resistance and use functions with the same exponent for tension and compression are investigated in [4, 11–13]. Anisotropic material models that take into account the difference in resistance and use power functions with different exponents for tension and compression are proposed in [14–16]. It is worth highlighting models that take into account the difference in material properties and use functions with the same exponent for tension, compression, and torsion [4, 17–19]. Significant difference of properties in torsion from those in tension and compression may be due to material anisotropy.

Recently, creep models have been developed taking into account the anisotropy and different material properties under tension and compression as well as material damageability [20], microstructure parameters (dislocation density) [21], and composite properties [22]. Creep models of anisotropic materials are being actively developed in geomechanics [23].

For a number of alloys, it has been experimentally shown that the rate of tension and compression can vary and be described by functions with different exponents [8, 24, 25]. In this paper, the model proposed in [7] that takes into account the difference between tensile and compressive resistances and uses a power function with different exponents for tension and compression is developed for orthotropic materials. Unlike the model described in [14], where transversely isotropic material is considered, the proposed model takes into account orthotropy. The proposed potential does not have a discontinuity [15] and quite accurately describes the uniaxial and biaxial tension and compression of material incompressible under creep [16].

1. MODEL OF ORTHOTROPIC MATERIAL WITH DIFFERENT PROPERTIES IN TENSION AND COMPRESSION

The orthotropy property and the difference in tensile and compressive resistances are described by the following model:

$$\eta_{ij} = \frac{\partial \Phi}{\partial \sigma_{ij}}, \qquad 2\Phi = \Phi_1 + \Phi_2 + (\Phi_2 - \Phi_1)\sin 3\xi; \tag{1}$$

$$\Phi_1 = T_1^{n_+ +1}/(n_+ + 1), \qquad \Phi_2 = T_2^{n_- +1}/(n_- + 1). \tag{2}$$

Here $\eta_{ij} = d\varepsilon_{ij}^c/dt$ are the components of the creep strain rate tensor, ε_{ij}^c and σ_{ij} are the components of the creep stress and strain tensors, and the invariant ξ is the angle which determines the type of stress state and takes into account different properties in tension and compression [4]:

$$\sin 3\xi = -\frac{9}{2}\,\frac{\bar\sigma_{kl}\bar\sigma_{lj}\bar\sigma_{kj}}{\sigma_i^3} \tag{3}$$

[$\bar\sigma_{kl}$ are the components of the stress deviator and $\sigma_i = (3\bar\sigma_{kl}\bar\sigma_{kl}/2)^{1/2}$ is the stress intensity]; Φ_1 and Φ_2 are the scalar potential functions of the stress tensor for tension and compression, respectively, and T_1 and T_2 are the quadratic forms of the stress tensor components:

$$\begin{aligned} T_1(\sigma_{ij}) &= (A_{11}^+(\sigma_{22}-\sigma_{33})^2 + A_{22}^+(\sigma_{33}-\sigma_{11})^2 + A_{33}^+(\sigma_{11}-\sigma_{22})^2 + 2A_{12}^+\sigma_{12}^2 + 2A_{23}^+\sigma_{23}^2 + 2A_{31}^+\sigma_{13}^2)^{1/2}, \\ T_2(\sigma_{ij}) &= (A_{11}^-(\sigma_{22}-\sigma_{33})^2 + A_{22}^-(\sigma_{33}-\sigma_{11})^2 + A_{33}^-(\sigma_{11}-\sigma_{22})^2 + 2A_{12}^-\sigma_{12}^2 + 2A_{23}^-\sigma_{23}^2 + 2A_{31}^-\sigma_{13}^2)^{1/2}; \end{aligned} \tag{4}$$

$$\begin{aligned} A_{11}^+ &= \Big((B_{22}^+)^{2/(n_+ +1)} + (B_{33}^+)^{2/(n_+ +1)} - (B_{11}^+)^{2/(n_+ +1)}\Big)/2, \\ 2A_{12}^+ &= 4(B_{12}^+)^{2/(n_+ +1)} - A_{11}^+ - A_{22}^+, \\ A_{11}^- &= \Big((B_{22}^-)^{2/(n_- +1)} + (B_{33}^-)^{2/(n_- +1)} - (B_{11}^-)^{2/(n_- +1)}\Big)/2, \\ 2A_{12}^- &= 4(B_{12}^-)^{2/(n_- +1)} - A_{11}^- - A_{22}^-. \end{aligned} \tag{5}$$

The remaining components A_{ij}^{+} and A_{ij}^{-} $(i,j=1,2,3)$ are obtained by cyclic permutation of indices. The constants B_{ii}^{+} and B_{ii}^{-} $(i=1,2,3)$ are characteristics of the one-dimensional steady-state creep process in tension and compression in three principal directions, respectively:

$$\eta_{ii}=\begin{cases} B_{ii}^{+}\sigma_{ii}^{n_+}, & \sigma_{ii}>0, \\ B_{ii}^{-}|\sigma_{ii}|^{n_--1}\sigma_{ii}, & \sigma_{ii}<0, \end{cases} \qquad i=1,2,3.$$

The constants B_{ij}^{+} and B_{ij}^{-} $(i\neq j)$ are the same characteristics in tension and compression, respectively, in three directions of the coordinate system obtained by rotation of the original coordinate system by an angle of 45°; n_+ and n_- are the exponents for one-dimensional creep in tension and compression.

Equations (1)–(5) lead to the following relations for an orthotropic material with the same tensile and compressive properties and for an isotropic material which has different tensile and compressive properties and for which the rate of tension and compression can be described by power functions with different exponents.

1.1. Orthotropic Material

If $B_{ij}^{+}=B_{ij}^{-}=B_{ij}$ $(i,j=1,2,3)$ and the exponent for creep does not depend on the sign of the applied load $(n_+=n_-=n)$, then from (1)–(5), it follows that $A_{ij}^{+}=A_{ij}^{-}$ $(i,j=1,2,3)$, $T_1=T_2=T$, and $\Phi_1=\Phi_2=\Phi$. For the components of the creep strain rates, we have

$$\eta_{ij}=\frac{\partial\Phi}{\partial\sigma_{ij}}, \qquad \Phi=\frac{T^{n+1}}{n+1}; \tag{6}$$

$$T(\sigma_{ij})=(A_{11}(\sigma_{22}-\sigma_{33})^2+A_{22}(\sigma_{33}-\sigma_{11})^2+A_{33}(\sigma_{11}-\sigma_{22})^2 + 2A_{12}\sigma_{12}^2+2A_{23}\sigma_{23}^2+2A_{31}\sigma_{13}^2)^{1/2}; \tag{7}$$

$$A_{11}=(B_{22}^{2/(n+1)}+B_{33}^{2/(n+1)}-B_{11}^{2/(n+1)})/2, \qquad 2A_{12}=4B_{12}^{2/(n+1)}-A_{11}-A_{22}. \tag{8}$$

Model (6)–(8) was proposed by Sosnin [9] to describe the orthotropic properties of materials under creep conditions. Although this model is well known, a few problems have been solved using this approach. This is due to the fact that obtaining model parameters for a specific material requires a large number of experiments to be performed. Validation of the obtained parameters and the model as a whole should be carried out for a complex stress state.

In [26], model (6)–(8) taking into account damageability is used to describe shell deformation based on momentless theory. One of the variants of model (6)–(8) with normalized constants A_{ij} was built in by the developers of ANSYS software into a finite element complex. Testing of the built-in model with the use of the Solid45 element by solving the problem of tension of a cubic specimen has shown that the calculated results for this model are in satisfactory agreement with the analytical solution [27]. For a complex stress state, the built-in model was used to evaluate the influence of the property of deformation normal to the sheet, which is weaker than deformation in the sheet plane, on the deflection in bending and torsion of plates of B95 alloy ($T=180$°C; thin sheets 6–10 mm thick) and 1163T alloy ($T=400$°C; plate 12 mm thick) [28, 29]. For the case of pure bending (torsion), a finite element solution obtained using the ANSYS software was compared with the results of two calculations, one of which uses integral quantities (curvature and moment) and the other reduces the resolving equations to a system of ordinary differential equations at partition points along the plate thickness. For 1163T alloy, the model was tested experimentally [29]. In [30], model (6)–(8) was used to study the effect of the resistance to creep deformation in a direction at an angle of 45° to the normal to the plate (i.e., in the shear direction), which is lower than the resistance to creep deformation in the plane of and normal to the sheet, on torsion process solid circular specimens (cut in the longitudinal direction and normal to the plate) of V95pchT2 alloy at $T=180$°C (plate thickness 50 mm) under the assumption of transversely isotropic properties of the alloy. In rods cut from plates in the longitudinal direction, deplanation of the cross section occurs [30]. In the case of cross-section deplanation, it is necessary to more accurately determine shear parameters for models [4, 13] based on experimental data on torsion with constrained deformation of the ends due to the presence of grips. In [31], model (6)–(8) is developed taking into account damage in a tensor formulation and is built in into the ANSYS package. Comparison of the calculated results with experimental data on uniaxial tension showed their satisfactory agreement.

In this case, we have $B_{ij}^{+} = B_{+}$, $B_{ij}^{-} = B_{-}$ $(i, j = 1, 2, 3)$, and $B_{+} \neq B_{-}$, $n_{+} \neq n_{-}$. Then, Eq. (5) lead to

$$2A_{12}^{+} = 2A_{23}^{+} = 2A_{31}^{+} = 3B_{+}^{2/(n_{+}+1)}, \qquad 2A_{12}^{-} = 2A_{23}^{-} = 2A_{31}^{-} = 3B_{-}^{2/(n_{-}+1)},$$

$$A_{11}^{+} + A_{22}^{+} = A_{22}^{+} + A_{33}^{+} = A_{33}^{+} + A_{11}^{+} = B_{+}^{2/(n_{+}+1)},$$

$$A_{11}^{-} + A_{22}^{-} = A_{22}^{-} + A_{33}^{-} = A_{33}^{-} + A_{11}^{-} = B_{-}^{2/(n_{-}+1)};$$

from (1)–(4) we obtain

$$\eta_{ij} = \frac{\partial \Phi}{\partial \sigma_{ij}}, \qquad 2\Phi(\sigma_i, \xi) = \Phi_1 + \Phi_2 + (\Phi_2 - \Phi_1)\sin 3\xi, \tag{9}$$

where $\Phi_1 = B_{+}\sigma_i^{n_{+}+1}/(n_{+}+1)$ and $\Phi_2 = B_{-}\sigma_i^{n_{-}+1}/(n_{-}+1)$. The creep constants B_{+}, n_{+} and B_{-}, n_{-} can be obtained in uniaxial tension and compression experiments, respectively, regardless of the direction in which the sample was cut from the plate ($\eta = B_{+}\sigma^{n_{+}}$ for $\sigma > 0$ and $\eta = B_{-}|\sigma|^{n_{-}-1}\sigma$ for $\sigma < 0$).

Model (9) was proposed and used in [7] to solve the pure torsion problems for a plate made of V95pchT2 alloy ($T = 180°$C; plate thickness 40 mm) under the assumption of a plane stress state. The solution was performed using the finite element algorithm included in the software package developed by the authors [7]. The obtained calculated results are in satisfactory agreement with experimental data. In [32], model (9) was used to develop a finite element algorithm built in into the MSC.Marc package for solving three-dimensional creep problems. The calculated results for torsion of a plate made of AK4-1 alloy ($T = 200°$C) are well consistent with experimental data and the calculated results for the model based on the concept of transformed stress space [33].

2. CONSTITUTIVE RELATIONS IN PARTICULAR CASES (PLANE STRESS STATE, TENSION, AND SHEAR)

We write the constitutive relations (1)–(5) in the case of a plane stress state. Since $\sigma_{33} = 0$, expression (3) is transformed to

$$\sin 3\xi = \frac{1}{2}\Big(\frac{I}{\sigma_i}\Big)^3 - \frac{3}{2}\,\frac{I}{\sigma_i},$$

where $I = \sigma_{11} + \sigma_{22}$ and $\sigma_i = (\sigma_{11}^2 + \sigma_{22}^2 - \sigma_{11}\sigma_{22} + 3\sigma_{12}^2)^{1/2}$ is the stress intensity.

We introduce the notation $\zeta = I/\sigma_i$. Then the expressions for the potential function (1) and quadratic forms (4) are written as

$$2\Phi = \Phi_1(T_1) + \Phi_2(T_2) + [\Phi_2(T_2) - \Phi_1(T_1)](\zeta^3 - 3\zeta)/2, \tag{10}$$

where

$$T_1 = ((A_{22}^{+} + A_{33}^{+})\sigma_{11}^2 + (A_{11}^{+} + A_{33}^{+})\sigma_{22}^2 - 2A_{33}^{+}\sigma_{11}\sigma_{22} + 2A_{12}^{+}\sigma_{12}^2)^{1/2},$$

$$T_2 = ((A_{22}^{-} + A_{33}^{-})\sigma_{11}^2 + (A_{11}^{-} + A_{33}^{-})\sigma_{22}^2 - 2A_{33}^{-}\sigma_{11}\sigma_{22} + 2A_{12}^{-}\sigma_{12}^2)^{1/2}.$$

For the components of the creep strain rate (1), we obtain

$$\begin{aligned}
\eta_{11} &= \lambda_1 T_1^{n_{+}-1}((A_{22}^{+} + A_{33}^{+})\sigma_{11} - A_{33}^{+}\sigma_{22}) + \lambda_2 T_2^{n_{-}-1}((A_{22}^{-} + A_{33}^{-})\sigma_{11} - A_{33}^{-}\sigma_{22}) \\
&\quad + \lambda_3\Big(\frac{T_2^{n_{-}+1}}{n_{-}+1} - \frac{T_1^{n_{+}+1}}{n_{+}+1}\Big)\,\frac{\sigma_{22}^2 - \sigma_{11}\sigma_{22} + 2\sigma_{12}^2}{\sigma_i^3}, \\
\eta_{22} &= \lambda_1 T_1^{n_{+}-1}((A_{33}^{+} + A_{11}^{+})\sigma_{22} - A_{33}^{+}\sigma_{11}) + \lambda_2 T_2^{n_{-}-1}((A_{33}^{-} + A_{11}^{-})\sigma_{22} - A_{33}^{-}\sigma_{11}) \\
&\quad + \lambda_3\Big(\frac{T_2^{n_{-}+1}}{n_{-}+1} - \frac{T_1^{n_{+}+1}}{n_{+}+1}\Big)\,\frac{\sigma_{11}^2 - \sigma_{11}\sigma_{22} + 2\sigma_{12}^2}{\sigma_i^3},
\end{aligned} \tag{11}$$

$$\eta_{12} = \lambda_1 T_1^{n_+-1}(2A_{12}^+\sigma_{12}) + \lambda_2 T_2^{n_--1}(2A_{12}^-\sigma_{12}) - \lambda_3\Big(\frac{T_2^{n_-+1}}{n_-+1} - \frac{T_1^{n_++1}}{n_++1}\Big)\frac{(\sigma_{11}+\sigma_{22})\sigma_{12}}{\sigma_i^3},$$

where

$$\lambda_1 = \frac{1}{2} - \frac{\zeta^3 - 3\zeta}{4}, \qquad \lambda_2 = \frac{1}{2} + \frac{\zeta^3 - 3\zeta}{4}, \qquad \lambda_3 = \frac{9}{4}(\zeta^2 - 1).$$

For an isotropic material with different tensile and compressive properties, expressions (10) and (11) are transformed to

$$2\Phi(\sigma_{11}, \sigma_{22}, \sigma_{12}) = \Phi_1(\sigma_i) + \Phi_2(\sigma_i) + [\Phi_2(\sigma_i) - \Phi_1(\sigma_i)](\zeta^3 - 3\zeta)/2,$$

$$\eta_{11} = \Phi_3(2\sigma_{11} - \sigma_{22}) + \Phi_4(\sigma_{22}^2 - \sigma_{11}\sigma_{22} + 2\sigma_{12}^2), \tag{12}$$

$$\eta_{22} = \Phi_3(2\sigma_{22} - \sigma_{11}) + \Phi_4(\sigma_{11}^2 - \sigma_{11}\sigma_{22} + 2\sigma_{12}^2), \quad \eta_{12} = 6\Phi_3\sigma_{12} - 2\Phi_4(\sigma_{11} + \sigma_{22})\sigma_{12}.$$

Here

$$\Phi_3 = \frac{1}{4}(B_+\sigma_i^{n_+-1} + B_-\sigma_i^{n_--1}) + \frac{1}{8}(B_-\sigma_i^{n_--1} - B_+\sigma_i^{n_+-1})(\zeta^3 - 3\zeta),$$

$$\Phi_4 = \frac{9}{8}\Big(\frac{B_-}{n_-+1}\,\sigma_i^{n_--2} - \frac{B_+}{n_++1}\,\sigma_i^{n_+-2}\Big)(\zeta^2 - 1).$$

In the case of simple tension ($\sigma_{11} = \sigma$ and $\sigma_{22} = \sigma_{33} = 0$), we have $\sigma_i = \sigma$, $\zeta = 1$, $\lambda_1 = 1$, and $\lambda_2 = \lambda_3 = 0$ and from (11) we get

$$\eta_{11} = T_1^{n_+-1}(A_{22}^+ + A_{33}^+)\sigma, \quad \eta_{22} = -T_1^{n_+-1}A_{33}^+\sigma, \quad \eta_{33} = -T_1^{n_+-1}A_{22}^+\sigma,$$

$$T_1 = \sqrt{A_{22}^+ + A_{33}^+}\,\sigma.$$

For orthotropic materials (6)–(8), we have

$$\eta_{11} = T^{n-1}(A_{22} + A_{33})\sigma, \quad \eta_{22} = -T^{n-1}A_{33}\sigma, \quad \eta_{33} = -T^{n-1}A_{22}\sigma,$$

$$T = \sqrt{A_{22} + A_{33}}\,\sigma.$$

For isotropic materials with different tensile and compressive properties, from (12) we have

$$\eta_{11} = B_+\sigma^{n_+}, \qquad \eta_{22} = \eta_{33} = -B_+\sigma^{n_+}/2.$$

In the case of uniform tension ($\sigma_{11} = \sigma_{22} = \sigma$ and $\sigma_{33} = 0$), we have $\sigma_i = \sigma$, $\zeta = 2$, $\lambda_1 = \lambda_3 = 0$, $\lambda_2 = 1$, and

$$\eta_{11} = T_2^{n_--1}A_{22}^-\sigma, \quad \eta_{22} = T_2^{n_--1}A_{11}^-\sigma, \quad \eta_{33} = -T_2^{n_--1}(A_{11}^- + A_{22}^-)\sigma,$$

$$T_2 = \sqrt{A_{11}^- + A_{22}^-}\,\sigma.$$

Uniform tension under stress σ in the x_1 and x_2 directions is equivalent to compression under stress σ in x_3 direction.

For orthotropic materials [relations (6)–(8)], we have

$$\eta_{11} = T^{n-1}A_{22}\sigma, \quad \eta_{22} = T^{n-1}A_{11}\sigma, \quad \eta_{33} = -T^{n-1}(A_{11} + A_{22})\sigma,$$

$$T = \sqrt{A_{11} + A_{22}}\,\sigma.$$

For isotropic materials with different tensile and compressive properties, from (12) we obtain

$$\eta_{11} = \eta_{22} = B_-\sigma^{n_-}/2, \qquad \eta_{33} = -B_-\sigma^{n_-}.$$

In the case of shear ($\sigma_{11} = \sigma_{22} = \sigma_{33} = 0$, $\sigma_{12} = \sigma$, and $\sigma > 0$), we have

$$\sigma_i = \sqrt{3}\,\sigma, \quad \zeta = 0, \quad \lambda_1 = \lambda_2 = 1/2, \quad \lambda_3 = -9/4,$$

$$\eta_{11} = \eta_{22} = \Big(\frac{T_1^{n_+ + 1}}{n_+ + 1} - \frac{T_2^{n_- + 1}}{n_- + 1}\Big)\frac{\sqrt{3}}{4\sigma}, \qquad \eta_{12} = (T_1^{n_+ - 1}A_{12}^{+} + T_2^{n_- - 1}A_{12}^{-})\sigma,$$

where $T_1 = \sqrt{2A_{12}^{+}}\,\sigma$ and $T_2 = \sqrt{2A_{12}^{-}}\,\sigma$.

For orthotropic materials [relations (6)–(8)], we have

$$\eta_{11} = \eta_{22} = \eta_{33} = 0, \qquad \eta_{12} = 2T^{n-1}A_{12}\sigma_{12}. \tag{13}$$

For isotropic materials with different tensile and compressive properties, from (12) we obtain

$$\eta_{11} = \eta_{22} = \frac{(\sqrt{3}\,)^{n_+ + 2}B_+\sigma^{n_+}}{4(n_+ + 1)} - \frac{(\sqrt{3}\,)^{n_- + 2}B_-\sigma^{n_-}}{4(n_- + 1)},$$

$$\eta_{12} = \frac{(\sqrt{3}\,)^{n_+ + 1}B_+\sigma^{n_+} + (\sqrt{3}\,)^{n_- + 1}B_-\sigma^{n_-}}{2}. \tag{14}$$

From (13) and (14), it follows that in the case of shear, the strains η_{11}, η_{22}, and $\eta_{33} = -(\eta_{11} + \eta_{22})$ are due to the different tensile and compressive properties of the material. For an isotropic material with different tensile and compressive properties which is described using a power function with exponent $n = n_+ = n_-$ and $B_+ \neq B_-$, relations (14) are simplified:

$$\eta_{11} = \eta_{22} = (\sqrt{3}\,)^{n+2}\,\frac{B_+ - B_-}{4(n+1)}\,\sigma^n, \qquad \eta_{12} = (\sqrt{3}\,)^{n+1}\,\frac{B_+ + B_-}{2}\,\sigma^n. \tag{15}$$

Note that in this case, the expressions for the shear strain rate η_{12} in (15) and in the model [1, 8] coincide.

3. TESTING OF THE ORTHOTROPIC MATERIAL MODEL WITH DIFFERENT PROPERTIES IN TENSION AND COMPRESSION

The calculated results for model (1)–(5) are compared with experimental data for AK4-1 transversely isotropic alloy. Experimental data on tension and compression of solid circular cylindrical specimens and on torsion of thin-walled tubular specimens cut from a plate 42 mm thick in the normal and in longitudinal directions at a temperature $T = 200°$C are given in [24].

Figure 1 shows the experimental time dependences of creep strain in tension at constant stresses $\sigma = 156.96$, 166.77, and 176.58 MPa for circular specimens cut at an angle of 45° to the normal to the plate (points *1–3*), in the longitudinal direction (points *4–6*) and transverse direction (points *7 and 8*), and in the direction normal to the plate (points *9* and *10*). It is seen that the properties of the alloy (creep strain rate) under tension in the plane of the plate in the longitudinal and transverse directions and in the direction normal to the plate are almost the same.

Figure 2 shows the experimental time dependences of creep strains in compression at a constant stress $\sigma = 176.58$, 186.36, and 196.20 MPa for specimens cut at an angle 45° to the normal to the plate (points *1–3*), in the longitudinal direction (points *4*) and transverse direction (points *5*), in the direction at an angle of 45° to the longitudinal direction (points *6*), and normal to the plate (points *7–9*). In both compression and tension, the creep strain rates of specimens cut in various directions in the plane of the plate (longitudinal and transverse directiona, and at an angle 45° to the longitudinal direction) and in the normal direction to the plate are close. Furthermore, the creep strain rate for the same stress $\sigma = 176.58$ MPa in compression in the plane of the plate and in the direction normal to it (points *5* and *7* in Fig. 2) is four times lower than that in tension (points *6*, *8*, and *10* in Fig. 1). The highest creep strain rate in both tension and compression is observed for specimens cut at an angle 45° to the normal to the plate; the creep rate is greater in tension than in compression.

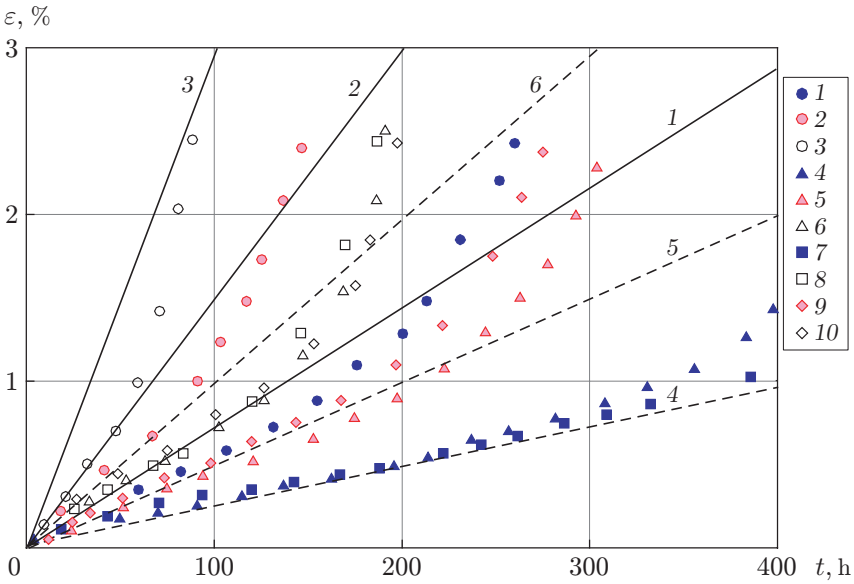

Fig. 1. Time dependences of creep strain for AK4-1 alloy specimens in tension at constant stress at $T = 200°$C and $\sigma = 156.96$ (*1*, *4*, and *7*), 166.77 (*2*, *5*, and *9*), and 176.58 MPa (*3*, *6*, *8*, and *10*): the points refer to the experimental data for specimens cut at an angle of 45° to the normal to the plate (*1–3*), specimens cut in the longitudinal direction (*4–6*), specimens cut in the transverse direction (*7* and *8*), and specimens cut normal to the plate (*9* and *10*); curves *1–3* are the approximations of calculated data with the parameters (16) and $n^+ = 12$ for tension of specimens cut at an angle of 45° normal to the plate, and curves *4–6* are the approximations of calculated data with the parameters (17) and $n^+ = 12$ for tension of specimens cut in the plane of the plate and normal to the plate.

To determine the parameters B_{ij}^+, n^+ and B_{ij}^-, n^-, we use the technique described in [34]. The experimental dependences shown in Figs. 1 and 2 are presented in the logarithmic coordinates $\ln\eta$–$\ln\sigma$ in Fig. 3. It is seen that the experimental points are grouped along curves *1–4*. The values of n^+ (curves *1* and *2*) and the values of n^- (curves *3* and *4*) obtained by the least squares method were averaged: $n^+ = 11.8$ and $n^- = 12.3$. To solve the torsion problem for rods using model (1), (2) for $n^+ \neq n^-$, it is necessary to use numerical methods. For $n^+ = n^-$, in some cases it is possible to obtain analytical solutions or estimates. Since the values of the creep exponents in tension and compression are almost equal: $n^+ \approx n^-$, we further assume that $n^+ = n^- = 12$. Approximation of the data shown in Fig. 3 yields the following parameter values:

$$B_{23}^+ = B_{31}^+ = 2.976 \cdot 10^{-35}\ \text{MPa}^{-n} \cdot \text{s}^{-1}\ \text{(curve } 1\text{)}; \tag{16}$$

$$B_{11}^+ = B_{22}^+ = B_{33}^+ = B_{12}^+ = 8.935 \cdot 10^{-35}\ \text{MPa}^{-n} \cdot \text{s}^{-1}\ \text{(curve } 2\text{)}; \tag{17}$$

$$B_{23}^- = B_{31}^- = 0.811 \cdot 10^{-35}\ \text{MPa}^{-n} \cdot \text{s}^{-1}\ \text{(curve } 3\text{)}; \tag{18}$$

$$B_{11}^- = B_{22}^- = B_{33}^- = B_{12}^- = 1.805 \cdot 10^{-35}\ \text{MPa}^{-n} \cdot \text{s}^{-1}\ \text{(curve } 4\text{)}. \tag{19}$$

The approximation straight lines obtained for these values of the constants are shown in Figs. 1 and 2.

3.1. Torsion of a Rod Cut Normal to the Plate

For torsion of rods cut normal to the plate by a constant moment, we have $\sigma_{11} = \sigma_{22} = \sigma_{22} = \sigma_{12} = 0$, $\sigma_{13} \neq 0$, and $\sigma_{23} \neq 0$. Elastic deformations are neglected. For the components of the creep strain rates, Eqs. (1)–(5) lead to

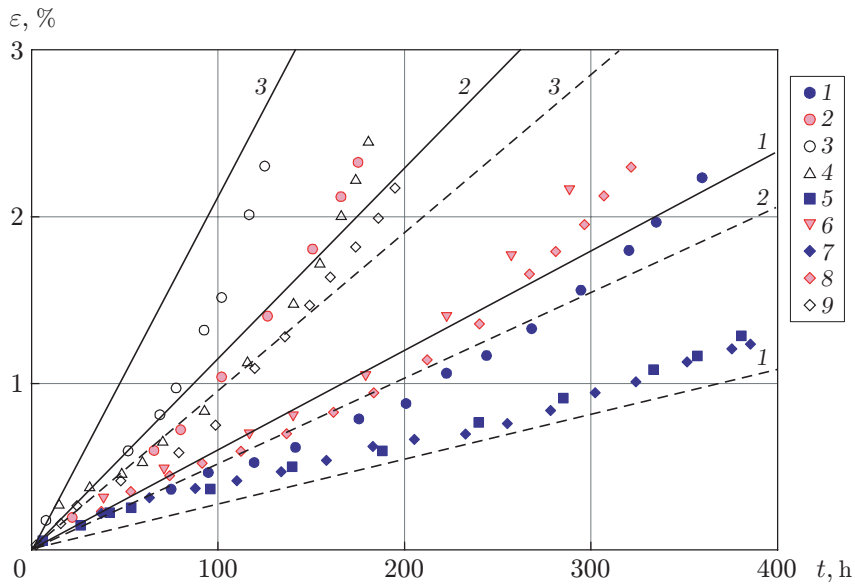

Fig. 2. Time dependence of creep strain for AK4-1 alloy specimens under compression at constant stress at $T = 200^\circ$C and $\sigma = 176.58$ (*1*, *5*, and *7*), 186.36 (*2*, *6*, and *8*), and 196.2 MPa (*3*, *4*, and *9*): the points refer to the experimental data for specimens cut at an angle 45° to the direction of the normal to the plate (*1–3*), specimens cut in the longitudinal direction (*4*), specimens cut in the transverse direction (*5*), specimens cut at an angle of 45° to the longitudinal direction in the plane of the plate (*6*), and specimens cut in the direction normal to the plate (*7–9*); the solid curves *1–3* are the approximations of the calculated data with parameters (18) and $n^- = 12$ for compression of specimens cut at an angle of 45° to the normal to the plate, and the dashed curves *1–3* are the approximations of the calculated data with the parameters (19) and $n^- = 12$ for compression of specimens cut in directions in the plane of the plate and normal to the plate.

$$\eta_{11} = \frac{\sqrt{3}}{4}\Big(\frac{T_1^{n_+ +1}}{n_+ + 1} - \frac{T_2^{n_- +1}}{n_- + 1}\Big)\frac{\sigma_{13}^2 - 2\sigma_{23}^2}{(\sigma_{13}^2 + \sigma_{23}^2)^{3/2}},$$

$$\eta_{22} = \frac{\sqrt{3}}{4}\Big(\frac{T_1^{n_+ +1}}{n_+ + 1} - \frac{T_2^{n_- +1}}{n_- + 1}\Big)\frac{\sigma_{23}^2 - 2\sigma_{13}^2}{(\sigma_{13}^2 + \sigma_{23}^2)^{3/2}}, \qquad (20)$$

$$\eta_{33} = \frac{\sqrt{3}}{4}\Big(\frac{T_1^{n_+ +1}}{n_+ + 1} - \frac{T_2^{n_- +1}}{n_- + 1}\Big)\frac{\sigma_{13}^2 + \sigma_{23}^2}{(\sigma_{13}^2 + \sigma_{23}^2)^{3/2}},$$

$$\eta_{12} = 0, \quad \eta_{13} = (A_{31}^+ T_1^{n_+ -1} + A_{31}^- T_2^{n_- -1})\sigma_{13}, \quad \eta_{23} = (A_{23}^+ T_1^{n_+ -1} + A_{23}^- T_2^{n_- -1})\sigma_{23},$$

where $T_1 = \sqrt{2A_{31}^+\sigma_{13}^2 + 2A_{23}^+\sigma_{23}^2}$ and $T_2 = \sqrt{2A_{31}^-\sigma_{13}^2 + 2A_{23}^-\sigma_{23}^2}$.

In view of (5) and (16)–(19), we have $A_{31}^+ = A_{23}^+$, $A_{31}^- = A_{23}^-$, $n^+ = n^- = n$, $T_1 = \sqrt{2A_{31}^+}\sqrt{\sigma_{13}^2 + \sigma_{23}^2}$, and $T_2 = \sqrt{2A_{31}^-}\sqrt{\sigma_{13}^2 + \sigma_{23}^2}$. Then, expressions (20) are rewritten as

$$\eta_{11} = D_1(\sigma_{13}^2 - 2\sigma_{23}^2)(\sigma_{13}^2 + \sigma_{23}^2)^{(n-2)/2}, \qquad \eta_{22} = D_1(\sigma_{23}^2 - 2\sigma_{13}^2)(\sigma_{13}^2 + \sigma_{23}^2)^{(n-2)/2},$$

$$\eta_{33} = D_1(\sigma_{13}^2 + \sigma_{23}^2)^{n/2}, \qquad \eta_{12} = 0,$$

$$\eta_{13} = D_2(\sigma_{13}^2 + \sigma_{23}^2)^{(n-1)/2}\sigma_{13}, \qquad \eta_{23} = D_2(\sigma_{13}^2 + \sigma_{23}^2)^{(n-1)/2}\sigma_{23},$$

where

$$D_1 = \frac{\sqrt{3}}{4(n+1)}\Big((2A_{31}^+)^{(n+1)/2} - (2A_{31}^-)^{(n+1)/2}\Big), \qquad D_2 = \frac{1}{2}\Big((2A_{31}^+)^{(n+1)/2} + (2A_{31}^-)^{(n+1)/2}\Big).$$

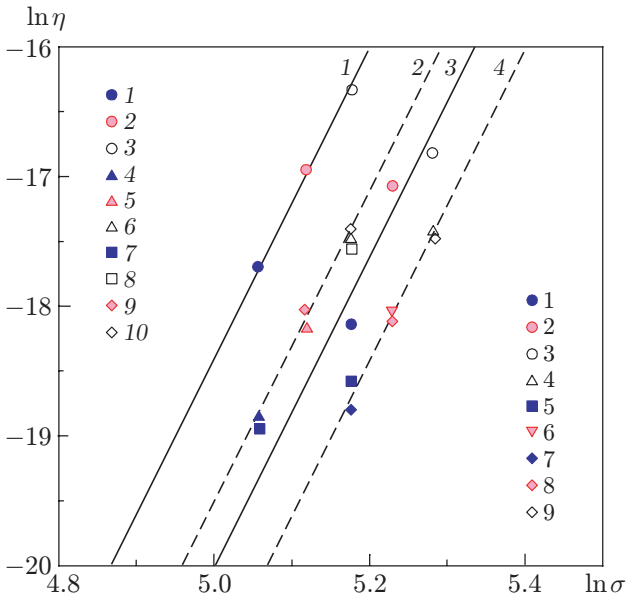

Fig. 3. Stress–strain curves in the logarithmic coordinates $\ln\eta - \ln\sigma$: curves *1 and 3* are the approximations of the calculated data for tension and compression of specimens cut at an angle of 45° to the normal to the plate, and curves *2 and 4* are the approximations of the calculated data for tension and compression of specimens cut in directions in the plane of the plate and normal to the plate; points *1–10* refer to the experimental data corresponding to points *1–10* in Fig. 1 and points 1–9 refer to the experimental data corresponding to points *1–9* in Fig. 2).

In the cylindrical coordinate system (r, φ, z) whose axis z coincides with the normal to the plate, the expressions for the shear strain rates take the form

$$\eta_{r\varphi} = \eta_{rz} = 0, \qquad \eta_{\varphi z} = D_2 \tau_{\varphi z}^n. \tag{21}$$

The torsional moment of a cylindrical cross-section rod with inner radius R_1 and outer radius R_2 ($R_1 \leqslant r \leqslant R_2$) is equal to

$$M = \int_0^{2\pi} \int_{R_1}^{R_2} \tau_{\varphi z} r^2 \, dr \, d\varphi. \tag{22}$$

Taking into account the equality $\eta_{\varphi z} = \theta r$, from (21) and (22), we obtain the following expression for the rate of change in the torsion angle of the rod per unit length θ [35]:

$$\theta = D_2 \Big(\frac{3 + 1/n}{2\pi} \frac{M}{R_2^{3+1/n} - R_1^{3+1/n}} \Big)^n. \tag{23}$$

In this case, the stress function such that $\tau_{\varphi z} = -\partial F / \partial r$ has the form

$$F(r) = \frac{(3 + 1/n) M R_2^{1+1/n} (1 - (r/R_2)^{1+1/n})}{2\pi (1 + 1/n)(R_2^{3+1/n} - R_1^{3+1/n})} = \Big(\frac{\theta}{D_2} \Big)^{1/n} \frac{1}{1 + 1/n} \, (R_2^{1+1/n} - r^{1+1/n}). \tag{24}$$

The shear stress is given by the formula

$$\tau_{\varphi z} = \frac{(3 + 1/n) M r^{1/n}}{2\pi (R_2^{3+1/n} - R_1^{3+1/n})}. \tag{25}$$

3.2. Torsion of a Rod Cut in the Longitudinal or Transverse Direction

For torsion of a rod cut in the longitudinal direction by a constant moment, we have $\sigma_{11} = \sigma_{22} = \sigma_{22} = \sigma_{23} = 0$, $\sigma_{12} \neq 0$, and $\sigma_{13} \neq 0$. For the components of the creep strain rates, from (1)–(5) we obtain

$$\eta_{11} = \frac{\sqrt{3}}{4}\Big(\frac{T_1^{n_+ +1}}{n_+ + 1} - \frac{T_2^{n_- +1}}{n_- + 1}\Big)\frac{\sigma_{12}^2 + \sigma_{13}^2}{(\sigma_{12}^2 + \sigma_{13}^2)^{3/2}},$$

$$\eta_{22} = \frac{\sqrt{3}}{4}\Big(\frac{T_1^{n_+ +1}}{n_+ + 1} - \frac{T_2^{n_- +1}}{n_- + 1}\Big)\frac{\sigma_{12}^2 - 2\sigma_{13}^2}{(\sigma_{12}^2 + \sigma_{13}^2)^{3/2}}, \tag{26}$$

$$\eta_{33} = \frac{\sqrt{3}}{4}\Big(\frac{T_1^{n_+ +1}}{n_+ + 1} - \frac{T_2^{n_- +1}}{n_- + 1}\Big)\frac{\sigma_{13}^2 - 2\sigma_{12}^2}{(\sigma_{12}^2 + \sigma_{13}^2)^{3/2}},$$

$$\eta_{12} = (A_{12}^+ T_1^{n_+ -1} + A_{12}^- T_2^{n_- -1})\sigma_{12}, \quad \eta_{13} = (A_{31}^+ T_1^{n_+ -1} + A_{31}^- T_2^{n_- -1})\sigma_{13}, \quad \eta_{23} = 0,$$

where $T_1 = \sqrt{2A_{12}^+\sigma_{12}^2 + 2A_{31}^+\sigma_{13}^2}$ and $T_2 = \sqrt{2A_{12}^-\sigma_{12}^2 + 2A_{31}^-\sigma_{13}^2}$.

In view of (5) and (16)–(19), we have $A_{12}^+ \neq A_{31}^+$ and $A_{12}^- \neq A_{31}^-$. For $n^+ = n^- = n$, the strain rates in the shear direction (26) can be expressed as

$$\eta_{12} = (A_{12}^+ T_1^{n-1} + A_{12}^- T_2^{n-1})\sigma_{12}, \qquad \eta_{13} = (A_{31}^+ T_1^{n-1} + A_{31}^- T_2^{n-1})\sigma_{13}. \tag{27}$$

Under the assumption of no constraint on the ends, the equilibrium equation for the rod in torsion is written as

$$\frac{\partial \sigma_{13}}{\partial x_3} + \frac{\partial \sigma_{12}}{\partial x_2} = 0. \tag{28}$$

The boundary condition on the cross-section contour has the form

$$\sigma_{13} n_3 + \sigma_{12} n_2 = 0. \tag{29}$$

The torsional moment is equal to

$$M = \iint\limits_S (\sigma_{13} x_2 - \sigma_{12} x_3)\, dx_2\, dx_3. \tag{30}$$

In this case, when solving the problem of torsion of a rod cut in the longitudinal direction, it must be borne in mind that shear deformations depend on the displacement of the points of the cross section along the axis of the rod (deplanation of the cross section) and the solution of the problem can be obtained using numerical calculation methods. However, the rate of change in the torsion angle can be estimated using the method described in [36]. In [36], the results of finite element calculations using the ANSYS package for a solid circular rod orthotropic in creep are compared with estimates obtained from the conditions of minimum additional dissipation and minimum total power. The difference between the torsion angle obtained from the condition of minimum additional dissipation (upper estimate) and the torsion angle calculated by the finite element method is of the order of 10%. Calculations show that for a thin-walled rod, this difference decreases.

A numerical solution of the problem of torsion of a rod with an arbitrary cross section (27)–(30) can be obtained by reducing the resolving relations to a differential equation for the deplanation $W(x_2, x_3)$ or for the stress function $F(x_2, x_3)$ such that $\sigma_{12} = \partial F/\partial x_3$ and $\sigma_{13} = -\partial F/\partial x_2$.

In the case of a doubly connected contour, the moment (30) is expressed in terms of the stress function $F(x_2, x_3)$ as follows [37]:

$$M = 2\iint\limits_{S_0} F\, dx_2\, dx_3 + 2F(C_1)S_1. \tag{31}$$

Here S_0 is the area bounded by the internal C_1 and external C_2 contours, S_1 is the area bounded by the contour C_1, and $F(C_1)$ is the value of the stress function on the contour C_1.

To obtain an upper estimate of the rate of change in the torsion angle, we use the condition of minimum additional dissipation [36, 37]. In view of (1), (27), and (31), this condition is written as

Results of calculating the rate of change in the torsion angle for annular cross-section specimens of AK4-1 alloy at $T = 200°\mathrm{C}$

Specimen number	Direction, in which the specimen is cut	M, N · m	$2R_1$, mm	$2R_2$, mm	$\theta \cdot 10^6$, rad/s^{-1}
1	3	55.67	18.013	20.010	7.845
2	3	41.00	18.220	19.938	1.117
3	3	180.03	10.030	19.980	10.140
4	1	56.12	17.985	20.002	4.511
5	1	50.30	17.992	20.000	1.274
6	1	47.32	18.000	20.000	0.640

$$I = \iint\limits_{S_0} \Big(\frac{T_1^{n+1} + T_2^{n+1}}{2(n+1)} - 2\theta F \Big)\, dx_2\, dx_3 - 2\theta F(R_1)\pi R_1^2 = \min. \tag{32}$$

We assume that the stress function has a form similar to (24):

$$F(x_2, x_3) = c\theta^{1/n} F_0(x_2, x_3) = c\theta^{1/n} \Big(1 - \Big(\sqrt{x_2^2 + x_3^2}\,/R_2 \Big)^{1+1/n} \Big)$$

or

$$F(r) = c\theta^{1/n} \Big(1 - (r/R_2)^{1+1/n} \Big) \tag{33}$$

(c is the constant to be determined). The z axis of the cylindrical coordinate system coincides with the x_1 direction. The function (33) with accuracy up to a factor is a solution of the torsion problem for a rod made of an isotropic material under steady-state creep conditions. This function satisfies the equilibrium equation (28), and on the external contour at $r = R_2$, it is equal to zero. Substituting (33) into (32), from the equation $dI/dc = 0$ we find the constant c for which (32) reaches a minimum:

$$\begin{gathered} c = \Big(\frac{J_1}{J_2} \Big)^{1/n}, \qquad J_1 = 2F_0(R_1)\pi R_1^2 + \iint\limits_{S_0} 2F_0\, dx_1\, dx_2, \\ J_2 = \frac{1}{2} \iint\limits_{S_0} \Big((2A_{12}^{+} F_{0.3}^2 + 2A_{31}^{+} F_{0.2}^2)^{(n+1)/2} + (2A_{12}^{-} F_{0.3}^2 + 2A_{31}^{-} F_{0.2}^2)^{(n+1)/2} \Big)\, dx_2\, dx_3. \end{gathered} \tag{34}$$

Here $F_{0.3} = \partial F_0/\partial x_3$ and $F_{0.2} = \partial F_0/\partial x_2$.

Taking into account (33) and (34), from (31) we find the rate of change in the torsion angle:

$$\theta = (M/(cJ_1))^n. \tag{35}$$

The stress value can be estimated approximately by the formula

$$\tau_{\varphi z} = -\frac{\partial F}{\partial r} = \Big(1 + \frac{1}{n} \Big) \frac{M}{J_1 R_2} \Big(\frac{r}{R_2} \Big)^{1/n}. \tag{36}$$

3.3. Comparison of Experimental Data and Calculated Results

Figure 4 shows the experimental time dependences of the torsion angle per unit length $\alpha = \theta t$ [24] for torsion by a constant moment at a temperature $T = 200°\mathrm{C}$ for cylindrical tubular specimens of AK4-1 alloy cut in the longitudinal direction and normal to the plate. For each specimen, the table shows the applied moment, inner and outer diameters, and the rate of change in the torsion angle calculated by formula (23) or (35) depending on the direction in which the specimen was cut.

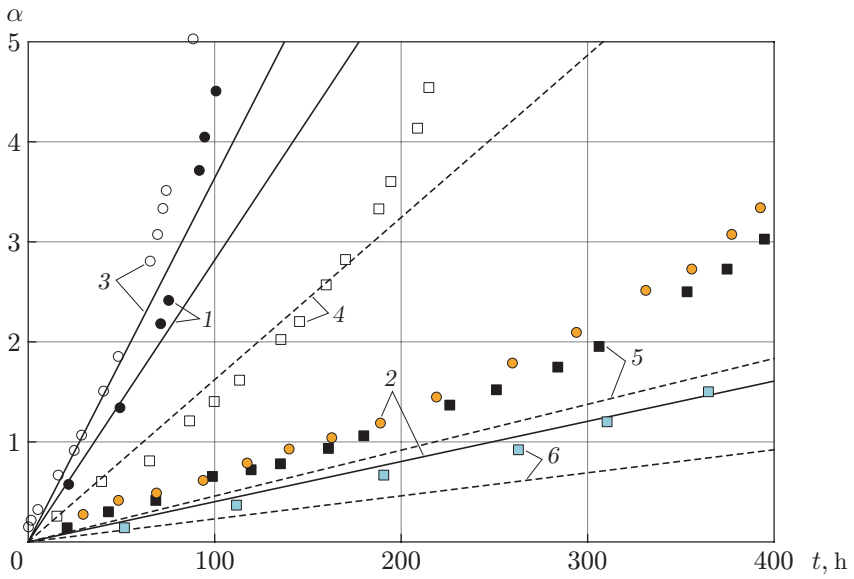

Fig. 4. Dependence of the torsion angle on time $\alpha(t)$ for cylindrical tubular specimens cut normal to the plate (*1–3*) and in the longitudinal direction (*4–6*): experimental points *1* and *2* refer to specimens 1 and 2 (see the table) with a wall thickness of 1 mm, points *3* to specimen 3 with a wall thickness of 5 mm, points *4–6* to specimens 4–6 with a wall thickness of 1 mm; the curves *1–3* refer to calculated results by formula (23) and curves *4–6* by formula (35).

The creep rate in tension and compression is greatest for AK4-1 alloy specimens cut at an angle of 45° to the normal to the plate. As a result, the rate of change in the torsion angle of the specimens cut normal to the plate is higher than the rate of change in the torsion angle of specimens cut in the longitudinal direction. This result is confirmed by experimental data. The stress intensity $\sigma_i = \sqrt{3}\,\tau_{\varphi z}$ calculated for $r = (R_1 + R_2)/2$ for specimen 1 by formula (25) and for specimen 4 by formula (36) is 170 MPa, while the torsion angles for these two specimens differ by a factor of two.

Thus, the results of calculations using the proposed model satisfactorily describe the experimental data.

CONCLUSIONS

The proposed orthotropic material model with different properties in tension and compression can be used to describe the creep process if the rates of tension and compression are described by functions with different exponents. Constitutive relations were obtained for the case of a plane stress state, and the cases of uniaxial and biaxial tension-compression for a material incompressible in creep were considered.

The proposed model was used to solve the problem of torsion by a constant moment at a temperature $T =$ 200°C for cylindrical tubular rods cut from a 42 mm thick plate of AK4-1 transversely isotropic alloy normal to the plate and in the longitudinal direction. Constitutive equations for torsion were obtained. The values of model parameters were found in uniaxial tension and compression experiments for solid circular specimens. For the same exponent for tension and compression, an analytical solution was obtained for the rate of change in the torsion angle of a rod cut normal to the transversely isotropic plate. For a rod cut in the longitudinal direction, an upper estimate of the rate of change in the torsion angle was obtained. The calculated results are in satisfactory agreement with experimental data.

REFERENCES

1. B. V. Gorev and A. F. Nikitenko, "On the Creep of Material with Different Characteristics in Tension and Compression," in *Dynamics of Continuous Media*, No. 6 (Inst. of Hydrodynamics, Sib. Branch, USSR Acad. of Sci., Novosibirsk, 1970), pp. 105–110.
2. B. V. Gorev, V. V. Rubanov, and O. V. Sosnin, "Construction of the Creep Equations for Materials with Different Extension and Compression Properties," Prikl. Mekh. Tekh. Fiz. **20** (4), 121–128 (1979) [J. Appl. Mech. Tech. Phys. **20** (4), 487–492 (1979)].
3. B. V. Gorev, V. V. Rubanov, and O. V. Sosnin, "On the Creep of Materials with Different Properties in Tension and Compression," Probl. Prochn., No. 7, 62–67 (1979).
4. I. Yu. Tsvelodub, *The Stability Postulate and Its Applications in Creep Theory of Metal Materials* (Inst. of Hydrodynamics, USSR Acad. of Sci., Novosibirsk, 1991) [in Russian].
5. I. Yu. Tsvelodub, "On the Creep of Materials with Different Properties in Tension and Compressive," in *Dynamics of Continuous Media*, Nos. 19/20 (Inst. of Hydrodynamics, Sib. Branch, USSR Acad. of Sci., Novosibirsk, 1974), pp. 147–155.
6. I. A. Banshchikova, A. E. Murav'eva, and I. Yu Tsvelodub, "Calculation of Plates Made of a Hardened Material with Different Resistance to Tension and Compression in Creep," Obrab. Metal. (Tekhnol., Oborud., Instr.) **4** (65), 68–77 (2014).
7. I. A. Banshchikova, B. V. Gorev, and I. Yu. Tsvelodub, "Creep of Plates Made of Aluminum Alloy under Bending," Prikl. Mekh. Tekh. Fiz. **48** (5), 156–159 (2007) [J. Appl. Mech. Tech. Phys. **48** (5), 751–754 (2007)].
8. I. A. Banshchikova and A. Yu. Larichkin, "Torsion of Solid Rods with Account for the Different Resistance of the Material to Tension and Compression under Creep," Prikl. Mekh. Tekh. Fiz. **59** (6), 123–134 (2018) [J. Appl. Mech. Tech. Phys. **59** (6), 1067–1077 (2018)].
9. O. V. Sosnin, "Anisotropic Creep of Materials," Prikl. Mekh. Tekh. Fiz., No. 6, 99–104 (1965) [J. Appl. Mech. Tech. Phys., No. 6, 67–70 (1965)].
10. J. Betten, *Creep Mechanics* (Springer-Verlag, Berlin–Heidelberg, 2008).
11. *Anisotropic Behaviour of Damaged Materials*, Ed. by J. J. Skrzypek and A. W. Ganczarski (Springer-Verlag, Berlin–Heidelberg, 2003). (Lect. Notes in Appl. and Comput. Mech., Vol. 9; DOI: 10.1007/978-3-540-36418-4.)
12. A. A. Zolochevsky, A. N. Sklepus, and S. N. Sklepus, *Nonlinear Mechanics of a Deformable Solid Body* (Business Investor Group, Kharkov, 2011).
13. G. Z. Voyiadjis and A. Zolochevsky, "Modeling of Secondary Creep Behavior for Anisotropic Materials with Different Properties in Tension and Compression," Int. J. Plasticity **14** (10/11), 1059–1083 (1998).
14. B. D. Annin, A. I. Oleinikov, and K. S. Bormotin, "Modeling of Forming of Wing Panels of the SSJ-100 Aircraft," Prikl. Mekh. Tekh. Fiz. **51** (4), 155–165 (2010) [J. Appl. Mech. Tech. Phys. **51** (4), 579–589 (2010)].
15. I. Yu. Tsvelodub, "Anisotropic Creep of Metallic Materials," Prikl. Mat. Mekh. **76** (4), 672–674 (2012).
16. I. Yu. Tsvelodub, "Construction of Constitutive Equations of Creep in Orthotropic Materials with Different Properties under Tension and Compression," Prikl. Mekh. Tekh. Fiz. **53** (6), 98–101 (2012) [J. Appl. Mech. Tech. Phys. **53** (6), 888–890 (2012)].
17. V. V. Tsvetkov, "Boundary-Value Creep Problems for Surface-Hardened Cylinders under Various Types of Quasistatic Loading," Abstract of Doct. Dissertation in Phys.-Math. Sci. (Samara State Tech. Univ., Samara, 2018).
18. B. V. Gorev, O. V. Sosnin, and I. V. Lyubashevskaya, "On the Creep of Materials with Different Properties in Tension and Compression," in *Proc. 4th All-Russian Conf. with International Participation, Samara, May 29–31, 2007* (Samara State Tech. Univ., Samara, 2007), Part 1, pp. 77–81.
19. A. Zolochevsky, A. Martynenko, and A. Kuhhorn, "Structural Benchmark Creep and Creep Damage Testing for Finite Element Analysis with Material Tension–Compression Asymmetry and Symmetry," Comput. Struct. **100/101**, 27–38 (2012); http://dx.doi.org/10.1016/j.compstruc.2012.02.021.
20. K. Naumenko and H. Altenbach, *Modeling High Temperature Materials behavior for Structural Analysis. Pt 1. Continuum Mechanics Foundations and Constitutive Models* (Springer, Switzerland, 2016); DOI: 10.1007/978-3-319-31629-1.
21. Y. Li, Z. Shi, J. Lin, et al., "A Unified Constitutive Model for Asymmetric Tension and Compression Creep-Ageing Behaviour of Naturally Aged Al–Cu–Li Alloy," Int. J. Plasticity **89**, 130–149 (2017); http://dx.doi.org/10.1016/j.ijplas.2016.11.007.

22. V. Kobelev, *Design and Analysis of Composite Structures for Automotive Applications: Chassis and Drivetrain* (John Wiley and Sons, Chichester, 2019).
23. M. Leoni, M. Karstunen, and P. A. Vermeer, "Anisotropic Creep Model for Soft Soils," Geotechnique **58** (3), 215–226 (2008).
24. B. V. Gorev and I. Zh. Masanov, "Deformation of Sheet Structural Aluminum Alloys and Plates in Creep Modes," Tekhnol. Mashinostr., No. 7, 13–20 (2009).
25. B. V. Gorev, I. V. Lyubashevskaya, V. A. Panamarev, and S. V. Iyavoyenen, "Description of Creep and Fracture of Modern Structural Materials Using Kinetic Equations in Energy Form," Prikl. Mekh. Tekh. Fiz. **55** (6), 132–144 (2014) [J. Appl. Mech. Tech Phys. **55** (6), 1020–1030 (2014)].
26. M. V. Gryazev, S. N. Larin, and S. S. Yakovlev, "Assessing the Effect of the Anisotropy of Mechanical Properties of a Workpiece on the Ultimate Capabilities of Isothermal Deformation of Hemispherical Parts in Creep," Izv. Tulsk. Gos. Univ., Tekh. Nauki, No. 2, 394–398 (2011).
27. I. A. Banshchikova, "Modeling of Anisotropic Creep by Using Hill's Theory," in *Zb. Radova Konferecncije MIT 2009* (Univ. Pristina, Kosovska Mitrovica; Inst. Comput. Technol., Novosibirsk, 2010), pp. 33–37.
28. I. A. Banshchikova, "Calculation of Double Curvature Plates Made of Anisotropic Alloys at Creep," Vest. Nizhegor. Univ., No. 4, Pt. 4, 1385–1387 (2011).
29. I. A. Banshchikova and V. A. Blinov, "Experimental and Theoretical Analysis of the Deformation of Transversely Isotropic Plates under Creep Conditions," Prikl. Mekh. Tekh. Fiz. **57** (3), 129–138 (2016) [J. Appl. Mech. Tech. Phys. **57** (3), 501–509 (2016).
30. I. A. Banshchikova, I. Yu. Tsvelodub, and D. M. Petrov, "Deformation of Structural Elements Made of Alloys with Reduced Resistance to Creep in the Shear Direction," Uchen. Zap. Kazan. Univ., Ser. Fiz.-Mat. Nauki **157** (3), 34–41 (2015).
31. C. M. Stewart, A. P. Gordon, Y. W. Ma, and R. W. Neu, "An Anisotropic Tertiary Creep Damage Constitutive Model for Anisotropic Materials," Int. J. Pressure Vessels Piping **88**, 356–364 (2011); DOI: 10.1016/j.ijpvp.2011.06.010.
32. S. N. Korobeynikov, A. I. Oleinikov, B. V. Gorev, and K. S. Bormotin, "Mathematical Simulation of Creep Processes in Metal Patterns Made of Materials with Different Extension Compression Properties," Vychisl. Met. Program.: Novye Vychisl. Tekhnol. **9** (1), 346–365 (2008).
33. B. V. Gorev and I. A. Banshchikova, "To Description of Creep Process and Fracture of Hardening Materials According to Kinetic Equations with Scalar Damage Parameter, Mathematical Modeling and Boundary-Value Problems," in *Proc. 7th All-Russian Sci. Conf. with International Participation, Samara, June 3–6, 2010* (Samara State Tech. Univ., Samara, 2010), Pt. 1, pp. 109–112.
34. O. V. Sosnin, B. V. Gorev, and A. F. Nikitenko, *Energy Version of Creep Theory* (Institute of Hydrodynamics, Sib. Branch, USSR Acad. of Sci., Novosibirsk, 1986) [in Russian].
35. I. A. Banshchikova, D. M. Petrov, and I. Yu. Tsvelodub, "Torsion of Circular Rods at Anisotropic Creep," J. Phys.: Conf. Ser. **722** (1), 012004 (2016).
36. I. A. Banshchikova, "Evaluation of the Stress–Strain State of Rod at Torsion from an Anisotropic Material in the Shear Direction at Creep," J. Phys.: Conf. Ser. **894**, 012006 (2017); DOI: 10.1088/1742-6596/894/1/012006.
37. L. M. Kachanov, *Creep Theory* (Fizmatgiz, Moscow, 1960) [in Russian].